

# High-Cycle Fatigue in a Hydraulic Turbine Runner

Andrea Carpinteri, Cristian Bagni, Daniela Scorza, Sabrina Vantadori

Dept of Civil-Environmental Engineering and Architecture, Viale G.P. Usberti 181/A, 43124 Parma (Italy), [sabrina.vantadori@unipr.it](mailto:sabrina.vantadori@unipr.it)

**ABSTRACT.** *A hydraulic turbine is an equipment where hot-formed blades are welded to band and crown by double-fillet welds. Decades of operating experience have shown that fatigue cracks develop in hydraulic turbine runners where both stress concentrations and material defects can be observed, as often occurs in the welded zones of such runners. In the present paper, a welded joint between the blade and the band or crown of a Francis turbine runner is considered, and the failure mechanism due to high-cycle fatigue loading produced by operational starts and stops is analysed. Such a welded joint can be idealised as a T-joint with a circular-shaped transition zone between blade and band (or crown), subjected to cyclic bending induced by the water action. A semi-elliptical surface crack is assumed to exist in the above transition zone, and the crack propagation is numerically examined by using the stress-intensity factor values obtained from finite element analyses. Experimental fatigue testing results are employed to substantiate these numerical estimations.*

## INTRODUCTION

Hydraulic power generation is a technology as important as both thermal power generation and nuclear power generation. The advantages of hydroelectric plants over fossil fuel plants are the following ones: longer life time, better efficiency rate (which is twice), and lower costs for maintenance and service. Further, a hydropower plant is a renewable and non-polluting source of energy, and can rapidly respond to changes in the power demand of the electric grid.

A Francis hydraulic turbine is an equipment where the runner is made by hot-formed blades welded to band and crown by double-fillet welds (Fig. 1a). Dynamic loads during the service life of the runner can cause failure and, therefore, represent a significant risk related to the structural reliability of the turbine [1, 2]. Decades of operating experience have shown that fatigue cracks develop in hydraulic turbine runners where both stress concentrations and material defects can be observed, as often occurs in the welded zones of such runners.

The welded connection between blade and band or crown can be considered as a T-joint subjected to bending (Fig. 1b): the vertical plate of such a joint represents the blade and the horizontal one the band or crown, whereas bending is induced by the steady (fluid pressure and centrifugal force) and unsteady (hydraulic load fluctuations due to irregular fluid flow and to start-up and shut-down operations) service loading. The level of stresses is intensified by the notch effect due to the T-joint geometry.

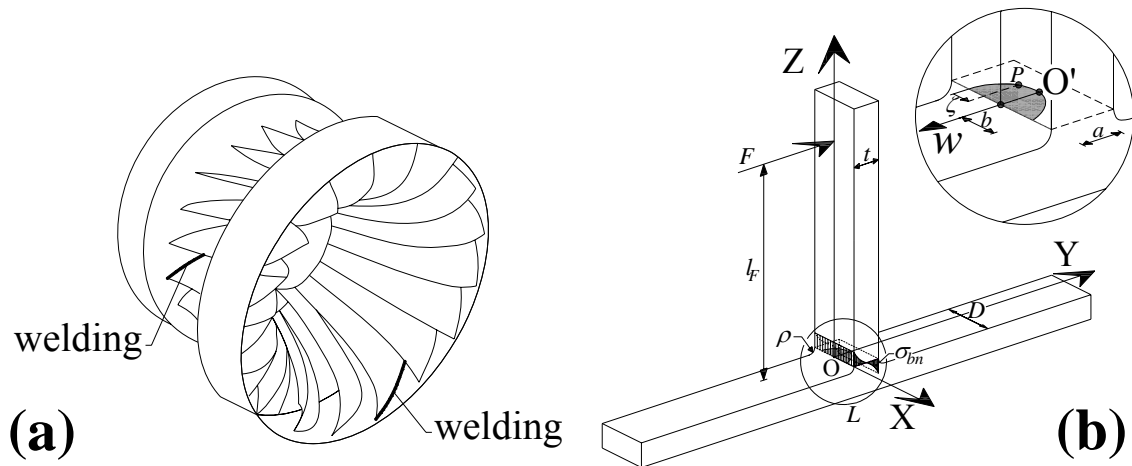


Figure 1. Welded connections between blade and band/crown (a); T-joint geometry (b).

A fracture mechanics approach is particularly suitable for the fatigue analysis of such a T-joint, in order to evaluate the crack growth rate of a surface defect detected at a given location (Fig. 1b). The failure mechanism is due to high-cycle fatigue loading produced by operational starts and stops: during a complete start-stop cycle, the loading goes from zero to a maximum value under service conditions, and back to zero. In the present paper, such a mechanism is numerically analysed through a procedure which consists of the following steps:

- (1) Calculation of the stress-intensity factors (SIFs) by means of three-dimensional finite element (FE) analyses related to a finite thickness plate under elementary stress distributions applied to the crack faces;
- (2) Evaluation of the stress field in the uncracked structural component;
- (3) Approximated SIF evaluation for the cracked structural component by employing the results deduced in step 1, and by applying the superposition principle and the power series expansion of the actual stress field determined in step 2;
- (4) Fatigue crack growth analysis by applying a theoretical model based on the Paris law.

Experimental fatigue tests available in the literature [3] are numerically simulated to substantiate the above procedure.

## SIF SOLUTIONS FOR FATIGUE CRACK GROWTH CALCULATION

The runner blade and its welded connection with the band or the crown can be idealized through a simple T-joint subjected to pure bending, as is shown in Fig. 1b. The joint examined herein is that used for fatigue testing reported in Ref. [3,4], and its geometry is scaled by a factor 2 with respect to the actual size of a common Francis turbine runner. The specimen width  $D$  is equal to 50 mm, the thickness blade  $t$  is equal to 20 mm, and the ratio between the thicknesses of blade and band (or crown) is equal to 5 / 6. The transition arc between blade and band (or crown) has a circular-arc shape, and the ratio

between the arc radius  $\rho$  and the blade thickness  $t$  is equal to 0.375. The bending loading in the nominal cross-section of the blade is produced by a transversal force  $F$ , located at  $Z=200$  mm level  $l_F$ , where  $F$  is the force applied by the load hydraulic cylinder of a fatigue machine on the specimen used in the experimental tests [3].

According to step 1 of the proposed procedure, a finite-thickness plate (with sizes  $t$  and  $D$ , equal to those of the plate representing the blade) containing a semi-elliptical surface crack (with semi-axes  $a$  and  $b$ , Fig. 1b) is here examined instead of the actual T-joint since, for relatively small cracks, the structural component geometry does not remarkably affect the stress-intensity factor values [4].

We consider four elementary stress distributions  $\sigma_{I(m)}$  directly applied (one at a time) on the defect faces, where  $I$  stands for Mode I and  $m$  represents the order of the monomial describing a given elementary stress distribution. Each stress distribution is characterized by zero value at point  $O'$  on the crack front (Fig. 1b) and unit value in correspondence to the outer surface of the plate (i.e. for coordinate  $w$  equal to  $a$ ):

$$\sigma_{I(m)} = \sigma_{ref(m)} \cdot \left(\frac{w}{a}\right)^m = \sigma_{ref(m)} \cdot \eta^m \quad \text{with } m = 0, \dots, 3 \quad (1)$$

where the elementary reference stress  $\sigma_{ref(m)}$  is equal to the unity. Three-dimensional linear FE analyses have been performed for such elementary loading conditions [5].

The stress-intensity factors,  $K_{I(m)}$  with  $m = 0, \dots, 3$ , for the elementary stresses can be evaluated along the defect front by applying the quarter-point FE nodal displacement correlation technique [6]. Then, the related dimensionless SIFs,  $K_{I(m)}^*$ , are computed as follows:

$$K_{I(m)}^* = \frac{K_{I(m)}}{\sigma_{ref(m)} \cdot \sqrt{\pi \cdot a}} \quad \text{with } m = 0, \dots, 3 \quad (2)$$

The crack configurations examined in step 1 are characterised by relative crack depth  $\xi = a/t$  ranging from 0.1 to 0.7, and crack aspect ratio  $\alpha = a/b$  ranging from 0.1 to 1.2.

According to step 2 of the proposed procedure, a two-dimensional FE analysis of the uncracked T-joint under bending is carried out by employing 632 eight-node plane strain elements in order to obtain the stress field in  $Z$ -direction [5]. Note that the force  $F$  does not induce only pure bending stresses, but also shear stresses. The values of such shear stresses are lower than 2% of the nominal surface stress under bending,  $\sigma_{ref(b)}$ , defined as the reference bending stress in the following:

$$\sigma_{ref(b)} = \frac{F \cdot l_F}{\frac{D \cdot t^3}{12} \cdot \frac{t}{2}} \quad (3)$$

and, therefore, the shear stresses can be neglected.

The Z-direction stress at the notch (location of the highest stress concentration,  $Z = 0$ ) of the uncracked T-joint is called  $\sigma_{bn}$ , where the subscripts  $b$  and  $n$  stand for “bending” and “notch”, respectively (Fig. 1b), whereas such a stress normalized with respect to the reference bending stress  $\sigma_{ref(b)}$  is called  $\sigma_{bn}^*$ . Such a normalized stress can be approximated through a power series expansion by performing a third-order ( $M = 3$ ) polynomial fitting of the obtained FEM results [5]:

$$\begin{aligned}\sigma_{bn}^*(w) &\cong \sum_{m=0}^{M=3} B_{m(bn)}^* \cdot \eta^m = \\ &= \left[ 1.17537 - 0.20514 \cdot a + 1.31425 \cdot (10)^{-2} \cdot a^2 - 4.38125 \cdot (10)^{-4} \cdot a^3 \right] + \\ &+ \left[ 0.20514 \cdot a - 2.62849 \cdot (10)^{-2} \cdot a^2 + 1.31437 \cdot (10)^{-3} \cdot a^3 \right] \eta + \\ &+ \left[ 1.31425 \cdot (10)^{-2} \cdot a^2 - 1.31437 \cdot (10)^{-3} \cdot a^3 \right] \eta^2 + \left[ 4.38125 \cdot (10)^{-4} \cdot a^3 \right] \eta^3\end{aligned}\quad (4)$$

According to step 3 of the proposed procedure, the stress-intensity factor related to a semi-elliptical surface crack located in correspondence to the highest stress concentration zone (notch) and characterised by the complex stress distribution  $\sigma_{bn}$  (Fig. 1b) is computed.

As is well-known, the SIF for a cracked body subjected to stresses (external or self-equilibrated) can be computed as the SIF due to only stresses acting on the defect faces, with the same magnitudes but opposite signs to those of the corresponding stresses in the body without crack [7-9]. In addition, the above complex stress distribution  $\sigma_{bn}$  is assumed to act on the faces of a semi-elliptical surface crack contained in a finite-thickness plate with sizes  $t$  and  $D$ .

By taking into account Eq.(1), the polynomial reported in Eq. (4) can be formally rewritten as a function of the monomials describing the elementary stress distributions:

$$\sigma_{bn}^*(w) \cong \sum_{m=0}^{M=3} B_{m(bn)}^* \cdot \eta^m = \sum_{m=0}^{M=3} \frac{B_{m(bn)}^*}{\sigma_{ref(m)}} \cdot \sigma_{I(m)} \quad (5)$$

According to the linear elastic fracture mechanics, the approximated dimensionless SIF along the front of a surface crack under the dimensionless stress distribution reported in Eq. (5) is defined as  $K_{I(bn)}^* = K_{I(bn)} / (\sigma_{ref(b)} \cdot \sqrt{\pi \cdot a})$ , and can be determined through the superposition principle [5]:

$$K_{I(bn)}^* = \sum_{m=0}^{M=3} B_{m(bn)}^* \cdot K_{I(m)}^* \quad (6)$$

## FATIGUE TESTING

The present Section briefly describes the experimental fatigue tests reported in Ref. [3]. The specimen geometry (representing the T-joint between Francis runner blade and ring or crown, Fig. 2a) and the loading condition (a transversal force applied by the load hydraulic cylinder) are able to represent the most critical situation for the Francis turbine runner, that is, the start-stop regime which occurs during arrest and re-start of such a runner.

The tested specimens were produced according to the standard manufacturing process for commercial turbine runners. The material employed is a martensitic-austenitic stainless steel, characterized by the following mechanical properties: ultimate tensile strength 945 MPa, yield strength 850 MPa, Young modulus, 200 GPa, Poisson ratio 0.3. Note that, due to manufacturing process inaccuracies, the geometric sizes of such specimens are not exactly equal to those of the examined T-joint.

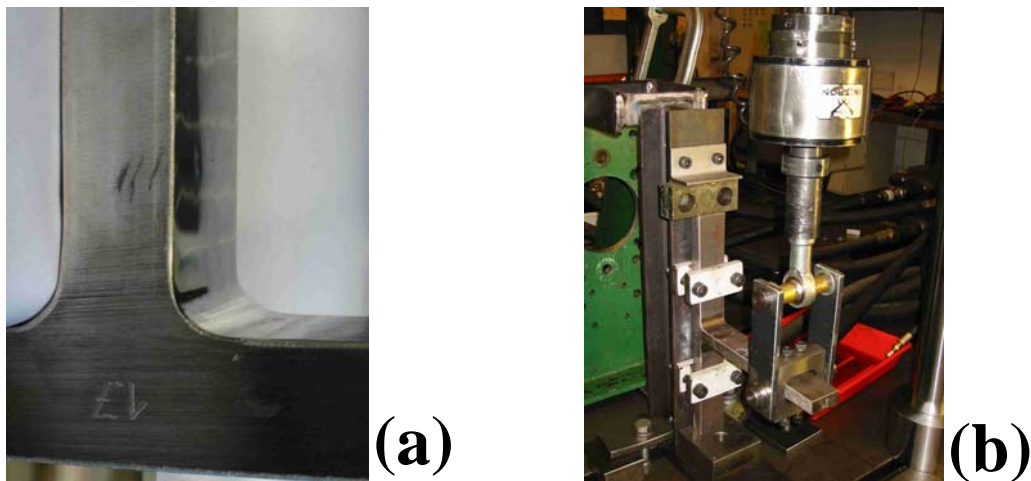


Figure 2. T-joint geometry specimen (a) and fatigue testing machine (b).

Each specimen was fixed to the frame of the fatigue-testing machine, as is shown in Figure 2b. A cyclic bending moment was applied to the thinner part (cantilever member) by the cylinder force  $F$ , producing maximum values of the reference bending stress,  $\sigma_{ref(b)}$ , equal to 911 MPa (cases A to D, details of which are presented in next Section) or 850 MPa (case E), with loading ratio  $R = 0.1$ . Such loading levels were chosen to obtain fatigue lives of magnitude order equal to  $10^4$  loading cycles, which is interesting from a practical hydropower-engineering point of view.

The growth of fatigue cracks starting at stress concentration locations has been monitored. In order to make the position of the crack front visible (beach marks), the crack surface was altered by temporarily propagating the crack at a lower growth rate. More precisely, the load sequence consisted of two consecutive blocks. The first one was the effective constant amplitude cyclic bending block containing 3.500 to 5.000 loading cycles, characterized by  $R = 0.1$ ,  $f = 3$  Hz and sinusoidal shape: this fatigue

loading produced crack propagation. The second cyclic loading block was the marker block:  $R$  was increased from 0.1 to 0.7, and the setup was maintained over 2.700 to 7.000 loading cycles of sinusoidal shape. The flaw size grows just a little during this second loading block and, therefore, the crack growth in such a phase can be neglected. For this reason, the number of cycles of the marker block is not taken into account when evaluating the specimen fatigue life.

These experimental fatigue bending tests on the T-joints [3] showed that a fatigue crack initiated at the surface of the welded zone (that is, at the location of the highest tensile stress concentration), and the beach marks of the growing crack had a semi-elliptical shape. The experimental data are reported in next Section and compared with numerical simulations carried out by the present authors.

## FATIGUE CRACK GROWTH: EXPERIMENTS AND SIMULATIONS

The above experimental tests are here numerically simulated, that is, the fatigue growth of a semi-elliptical surface flaw in a plate is analysed by applying a two-parameter theoretical model [10] based on the Paris law. According to such a model, the crack front with semi-axes  $a$  and  $b$  (Fig. 1b) grows, after one loading cycle, to a new configuration described by the following expression:

$$\frac{x^2}{(b^*)^2} + \frac{y^2}{(a^*)^2} = 1 \quad (7)$$

where  $a^*$  and  $b^*$  are the semi-axes of the surface flaw after one loading cycle. The model assumes that the surface crack under Mode I loading conditions keeps a semi-elliptical shape during propagation: such an assumption, frequently made in the literature, has proved to yield reliable results for different specimen geometries, and is in agreement with the experimental results here examined.

The crack growth rate at the crack front location, for a given crack configuration characterized by the two dimensionless geometrical parameters  $\xi = a/t$ ,  $\alpha = a/b$ , can be expressed by the Paris law:

$$\frac{da}{dN} = C(\Delta K_I)^m \quad (8)$$

where  $C$  and  $m$  are material constants.

By employing the SIF values  $K_{I(bn)}$  (Ref. [5]) and applying Eq. (8) at two points (on the crack front) with the normalised coordinate  $\zeta^* = \zeta/b$  (see Fig. 1b) equal to 0.1 and 1.0, respectively, the fatigue crack growth paths are numerically determined for the initial surface flaw parameters and the loading condition such as those of the above experimental tests. Further, the material constants  $m$  and  $C$  (Eq. (8)) are assumed to be equal to 3.22 and  $6.67 \cdot 10^{-13}$ , respectively (with  $da/dN$  expressed in  $\text{m} \cdot \text{cycle}^{-1}$  and  $\Delta K_I$  in  $\text{MPa} \cdot \text{m}^{1/2}$ ), which are the experimental values for the material tested.

The numerical diagram of  $\alpha$  against  $\xi$  is shown in Fig. 3, for five different initial cracks (see continuous and dashed curves). It can be observed that fatigue crack growth paths tend to converge to a common inclined asymptote.

Experimental results [3] are also reported in Fig. 3: the solid symbols indicate the values of  $\alpha$  and  $\xi$  for the semi-ellipses that best fit the beach marked crack fronts during the fatigue tests examined. The numerical fatigue crack growth paths are in satisfactory agreement with the experimental results, especially for the cases from B to E.

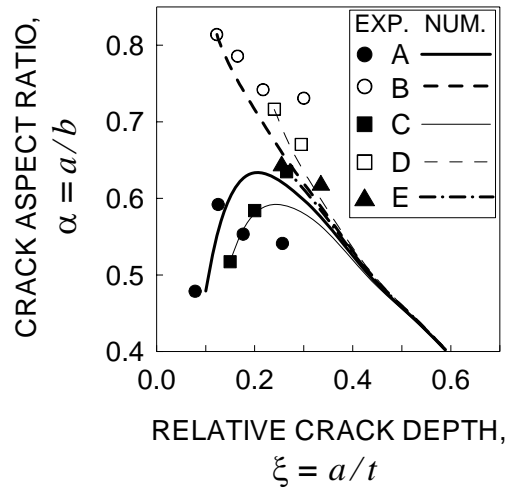


Figure 3. Diagram of  $\alpha$  vs  $\xi$ . Experimental results are also reported (solid symbols).

Figure 4 displays the loading cycle number  $N$  against the relative crack depth  $\xi$ , together with beach mark data from experimental tests. By comparing numerical and experimental results, it can be observed that the proposed model is able to correctly estimate the value of  $N$ .

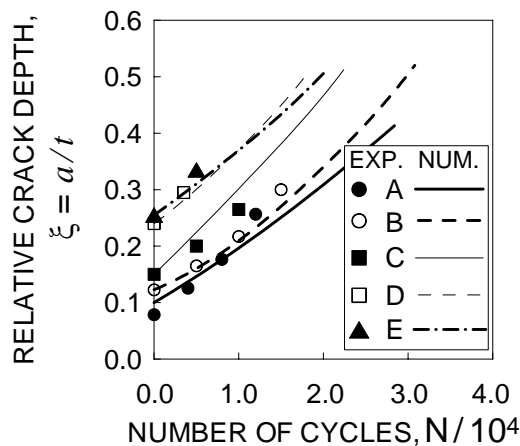


Figure 4. Diagram of  $N$  vs  $\xi$ . Experimental results are also reported (solid symbols).

## CONCLUSIONS

In the present paper, the fatigue behaviour of a welded T-joint with a surface crack has been examined. First of all, a finite-thickness plate with a semi-elliptical surface flaw has numerically been analysed. Then, approximate values of SIF for the cracked T-joint under bending have been determined. Such SIF values have been used for fatigue crack growth simulations by also applying a two-parameter model based on the Paris law.

Experimental fatigue test results on T-jointed specimens, available in the literature, have been compared with the numerical results, and the agreement seems to be quite satisfactory, that is, the proposed numerical procedure seems to be promising for fatigue life assessment of structural components with semi-elliptical surface defects.

## REFERENCES

1. Fisher, R.K. (2002). In: *Proceedings of the XXI IAHR "Symposium on Hydraulic Machinery and Systems"*, Lausanne, Switzerland.
2. Frunzăverde D., Muntean S., Mărginean G., Câmpian V., Marşavina L., Terzi R., Şerban V. (2010). In: *IOP Conference series "Earth and Environmental Science"* **12**, pp. 1-10.
3. Huth H-J. (2004). PhD thesis, Norwegian University of Science and Technology, Trondheim, Norway.
4. Carpinteri A., Brighenti R., Huth H.-J., Vantadori S. (2005). *Int. J. Fat.* **27**, 59-69.
5. Carpinteri A., Vantadori S. (2012). Submitted to *Engng Fract. Mech.*.
6. Lim I.L., Johnston I.W., Choi S.K. (1992). *Com. App. Num. Meth.* **8**, 291-300.
7. Carpinteri A., Brighenti R., Vantadori S. (2004). *Engng Frac. Mech.* **71**, 485-499.
8. Carpinteri A., Brighenti R., Vantadori S. (2006). *Int. J. Mech. Sci.* **48**, 638-649.
9. Carpinteri A., Brighenti R., Vantadori S. (2009). *Int. J. Press. Vess. & Pip.* **86**, 443-453.
10. Carpinteri A. (1993). *Int. J. Fatigue*, **15**, 21-26.